

Aggregation of magnetic holes in a rotating magnetic field

Jozef Černák*

Institute of Physics, P. J. Šafárik University in Košice, Jesenná 5, SK-04000 Košice, Slovak Republic

Geir Helgesen

Physics Department, Institute for Energy Technology, NO-2027, Kjeller, Norway

(Received 20 June 2008; published 8 December 2008)

We experimentally investigated field-induced aggregation of nonmagnetic particles confined in a magnetic fluid layer when rotating magnetic fields were applied. After application of a magnetic field rotating in the plane of the fluid layer, the single particles start to form two-dimensional clusters, like dimers, trimers, and more complex structures. These clusters aggregated again and again to form bigger clusters. During this nonequilibrium process, a broad range of cluster sizes was formed, and the scaling exponents z and z' of the number of clusters $N(t) \sim t^{-z'}$ and average cluster size $S(t) \sim t^z$ were calculated. The process could be characterized as diffusion-limited cluster-cluster aggregation. We found that all sizes of clusters that occurred during an experiment fall on a single curve, as the dynamic scaling theory predicts. However, the characteristic scaling exponents z' , z and crossover exponents Δ were not universal. A particle tracking method was used to find the dependence of the diffusion coefficients D_s on cluster size s . The cluster motions show features of Brownian motion. The average diffusion coefficients $\langle D_s \rangle$ depend on the cluster size s as a power law $\langle D_s \rangle \propto s^\gamma$ where values of γ as different as $\gamma = -0.62 \pm 0.19$ and $\gamma = -2.08 \pm 0.51$ were found in two of the experiments.

DOI: [10.1103/PhysRevE.78.061401](https://doi.org/10.1103/PhysRevE.78.061401)

PACS number(s): 82.70.Dd, 83.10.Tv, 75.50.Mm, 89.75.Da

I. INTRODUCTION

Colloidal aggregation phenomena are interesting subjects of study for both theoretical and technological reasons. In systems with short-range interactions the main aggregation features are well understood [1]. The diffusion-limited cluster-cluster aggregation (CCA) model [2,3] and dynamic scaling theory [4] explain well the scaling properties during aggregation. It has been found that these models, initially developed for systems with short-range interactions, can be used in systems where dipole-dipole interaction is dominant, for example aggregation of magnetic microspheres [5,6], aggregation of nanoparticles in magnetic fluids [7], and aggregation of magnetic holes [8]. These experimental results show scaling of the significant parameters and features typical of CCA. On the other hand, the corresponding exponents may deviate slightly from the values predicted by the model, and the reasons for this are still not understood.

Our previous results [8] served as a motivation for this study. Aggregation of magnetic holes in constant magnetic fields was interpreted in the frames of the CCA model and dynamic scaling theory. The scaling exponent $z \approx 0.42$ for the cluster size dependence $S(t) \sim t^z$ was found for particles of diameters $d = 1.9$ and $4 \mu\text{m}$. This value of the exponent is slightly lower than exponent values predicted by theory ($z = 0.5$) [2] or found in computer simulations ($z = 0.5$ for isotropic and 0.61 for anisotropic aggregation) [9]. Under certain experimental conditions (i.e., particles with larger diameter $d = 14 \mu\text{m}$) the exponent z was close to or lower than the exponent value corresponding to a transition from two-dimensional (2D) to 1D aggregation ($z = 1/3$). Based on these optical observations, we know that for a constant mag-

netic field clusters move in 2D but they grow only in one dimension.

Constant magnetic fields induce the formation of long chains of particles [6,8]. In order to determine the correct scaling exponents, one may take into account hydrodynamic effects [9]. Here, we will show that by applying rotating magnetic fields we ensure quasi-isotropic properties inside the magnetic fluid (MF) sample. In this case clusters can move in 2D space and can grow as 2D compact objects, and thus the hydrodynamic corrections should be less important.

The dynamic properties of a few magnetic holes [10] in rotating magnetic fields show interesting phenomena, for example nonlinear response of bound pairs of magnetic holes [11], complex braid dynamics [12], and equilibrium configurations of rotating particles without contact between particles [13]. In a precessing magnetic field, paramagnetic particles dispersed in a drop of water self-assemble into two-dimensional viscoelastic small clusters [14].

In the present study, field-induced aggregation of many magnetic holes has been observed. In Sec. II the experimental equipment and the methods used are described. Section III deals with the results concerning the determination of the scaling exponents and characterization of the diffusion behavior of individual clusters by tracking of their motions. In Sec. IV we summarize the general features and try to explain the nonuniversal scaling exponents. Our conclusions follow in Sec. V.

II. MICROSCOPIC OBSERVATIONS

The experimental setup shown in Fig. 1 consists of an optical microscope (Nikon Optiphot), two pairs of coils, and a carefully prepared sample confined to a thin layer. Alternating currents were supplied to the coils in order to produce a magnetic field rotating in the horizontal plane of the

*jozef.cernak@upjs.sk

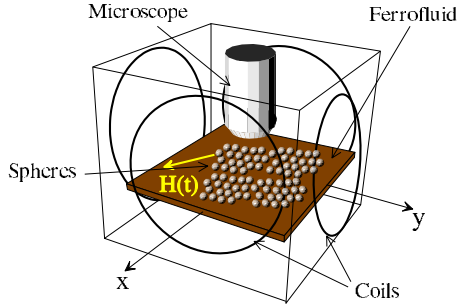


FIG. 1. (Color online) Experimental setup used to study aggregation of magnetic holes. A rotating magnetic field $\mathbf{H}(t)$ is applied in the plane of the magnetic fluid.

sample. Microscopic observations were captured by a charge-coupled device camera (Q-Imaging Micropublisher 5) with resolution 2560×1920 pixels.

A layer of magnetic fluid (ferrofluid) of thickness approximately $50 \mu\text{m}$ was confined between two glass plates and sealed. The sample size was about $20 \times 20 \text{ mm}^2$. A very low concentration of spherical particles with diameter $50 \mu\text{m}$ was used as spacer in order to have an even sample thickness. The kerosene-based ferrofluid [15] had the following physical properties: density $\rho = 1020 \text{ kg m}^{-3}$, susceptibility $\chi = 0.8$, saturation magnetization $M_s = 20 \text{ mT}$, and viscosity $\eta = 6 \times 10^{-3} \text{ N s m}^{-2}$. Monodisperse polystyrene microspheres of diameter $d = 3 \mu\text{m}$ were dispersed in the MF layer in order to create magnetic holes in the presence of magnetic fields.

Without a magnetic field the particles are homogeneously dispersed in the layer and they can move freely. After some time, a very low fraction of particles may randomly join to other particles and a few dimers were observed [10]. Their volume fraction is very low in comparison with the volume fraction of single particles. However, before the application of the rotating magnetic field, a short magnetic field pulse perpendicular to the sample (coils are not shown in Fig. 1) was applied in order to destroy these dimers and to create a monodisperse initial size distribution of particles. This initial stage of the experiment is not shown in Fig. 2.

The rotating magnetic field $\mathbf{H}(t) = (H_x, H_y)$ within the x - y plane had the components: $H_x = H \sin(\omega t)$ and $H_y = H \sin(\omega t + \pi/2)$. The amplitude of the magnetic field was constant, $H = 793 \text{ A m}^{-1}$, and the angular velocity $\omega = 251 \text{ s}^{-1}$. The effective volume susceptibility including the demagnetization correction for spherical magnetic holes was $\chi_{\text{eff}} = \chi / (1 + 2\chi/3) = 0.63$. The dimensionless interaction strength parameter [8] was $\lambda \approx 90$. Here, $\lambda = U_{\text{max}}^{\text{dip}} / kT$, where $U_{\text{max}}^{\text{dip}}$ is the maximal dipolar energy of two dipolar particles joined together, k is Boltzmann's constant, and T is the temperature, $T \approx 293 \text{ K}$. Thus, the dipole-dipole interaction among magnetic holes was dominant relative to the thermal fluctuations.

The rotating magnetic field caused an aggregation of the microspheres. The process took place via the joining of single particles into dimers and trimers and the formation of 2D clusters consisting of many particles. These new clusters aggregated again and formed bigger clusters. A typical aggregation dynamics is shown in Fig. 2. A few samples with approximately the same layer thickness were investigated.

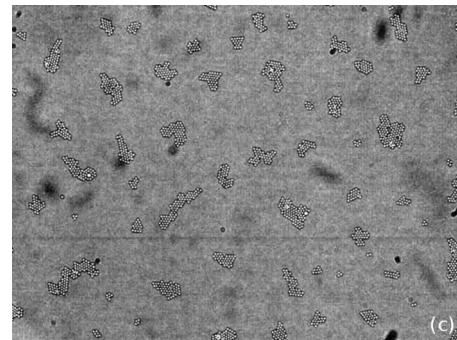
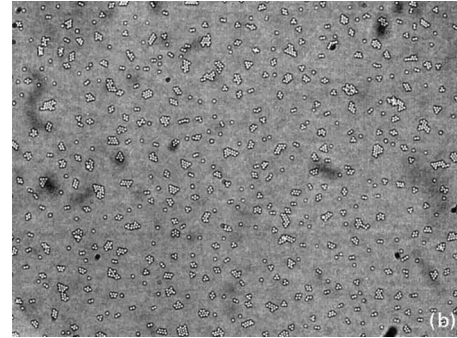
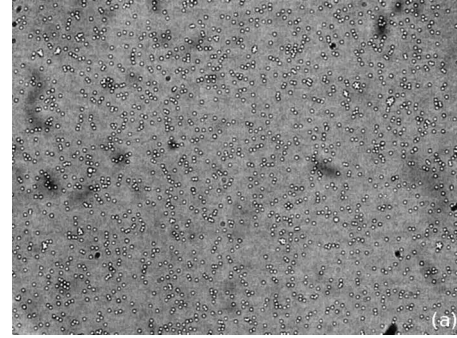


FIG. 2. Optical micrographs of aggregation of nonmagnetic microspheres with diameter $d = 3 \mu\text{m}$ in magnetic fluid at different times $t =$ (a) 0, (b) 210, and (c) 4470 s after the magnetic field was switched on. The applied rotating magnetic field had amplitude $|\mathbf{H}| = 793 \text{ A m}^{-1}$ and frequency $f = 40 \text{ Hz}$. The images cover a sample area of about $368 \times 274 \mu\text{m}^2$.

The volume fractions of particles were low, in the range $\phi = 0.0014 - 0.0064$.

In order to analyze the digital images, a C programming language code and open graphical libraries were used. Several thousand digital pictures have been analyzed in a distributed manner in a computational grid. We analyzed the motion of individual particles during aggregation using our own tracking algorithms written in the PYTHON programming language.

III. RESULTS

Microspheres confined in a magnetic fluid layer without a magnetic field behave as nonmagnetic particles dispersed in a fluid. They perform random Brownian motion. In this case, aggregation events are rare due to the low particle concen-

tration. Thus, in the initial stage of the experiments [Fig. 2(a)] the microspheres are homogeneously dispersed in the layer of MF and the cluster size distribution is unimodal.

After the external magnetic field is turned on, the microspheres behave as interacting magnetic holes. They have induced magnetic moments which are oriented oppositely to the direction of the external magnetic field. When the energy of the dipole-dipole interaction between two arbitrary spheres is larger than the thermal energy of the spheres, as quantified by the dimensionless interaction strength $\lambda \approx 90$ in the present case, the field-induced aggregation starts.

During the aggregation, complex motions of microspheres and clusters consisting of many microspheres were observed. Clusters containing regularly ordered particles were formed and small irregular clusters relaxed relatively quickly to highly ordered structures. Based on the optical observation, the complex modes of motion of microspheres and clusters may be classified as (i) the joining of two clusters together followed by a very slow relaxation of the microspheres in the new cluster into a more ordered structure; (ii) extremely slowly swiveling of all clusters in the same direction as the rotating magnetic field, followed by packing into a compact disk form; and (iii) small random motions of the clusters induced by random forces resulting from interactions with the local cluster environment.

We have observed that clusters of all sizes can join together and form bigger clusters, which is the basic feature of cluster-cluster aggregation. The cluster-cluster aggregation model [2] predicts the scaling properties of the total number of clusters $N(t)$ and the mean cluster size $S(t)$. The total number of clusters is defined as $N(t) = \sum_s n_s(t)$, where $n_s(t)$ is number of clusters of size s at time t . The mean cluster size $S(t)$ is defined as

$$S(t) = \frac{\sum_s n_s(t) s^2}{\sum_s n_s(t) s}, \quad (1)$$

where s is the cluster size. In our case the cluster size s is given by the number of particles that belong to the cluster.

The aggregation process shown in Fig. 2 was studied in more detail. In Fig. 3(a) one can see that the total number of clusters $N(t)$ and mean cluster size $S(t)$ show power law dependencies $N(t) \sim t^{-z'}$ and $S(t) \sim t^z$. This behavior was found for the time interval $t=200-3400$ s. The scaling exponents were calculated to be $z' = 0.65 \pm 0.01$ and $z = 0.64 \pm 0.01$.

Based on dynamic scaling theory [4] all cluster numbers $n_s(t)$ can be scaled into a single, universal curve or scaling function $g(x)$, defined as

$$n_s(t) \sim s^{-2} g(s/t^\tau). \quad (2)$$

It is expected that $g(x) \sim x^\Delta$ for $x \ll 1$.

All the cluster number curves $n_s(t)$ during the time interval $t=200-3400$ s were found to fall onto the single curve shown in Fig. 3(b). From this curve the characteristic scaling exponent was fitted to be $\Delta = 1.44 \pm 0.08$.

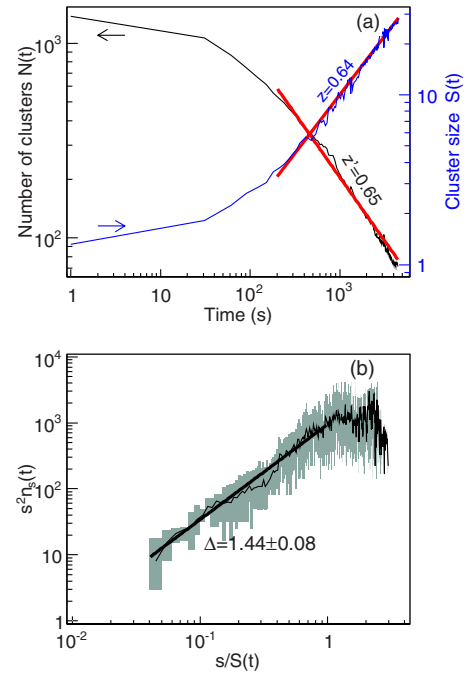


FIG. 3. (Color online) (a) The total number of clusters $N(t)$ and the mean (weight average) cluster size $S(t)$ (in units of number of spheres) versus time. (b) The scaling function $g(x) = s^2 n_s(t)$ obtained from the cluster size distributions $n_s(t)$ during the time interval $t = 200-3400$ s.

However, we measured several samples and some of these showed a different behavior. Their scaling exponents z, z' and crossover exponent Δ were different from the results presented above. Typical results for a sample that shows a different type of behavior are shown in Fig. 4(a). Here, the scaling exponents were found to be $z' = 0.40 \pm 0.03$ and $z = 0.34 \pm 0.02$. Similarly to the case discussed above, the cluster numbers $n_s(t)$ ($t=200-80000$ s) that were measured for this sample could be scaled onto a single curve as shown in Fig. 4(b), but the scaling exponent Δ was nearly twice as large as in the former case, $\Delta = 2.75 \pm 0.06$. Also in this case the visible dynamic behavior was consistent with diffusion-limited cluster-cluster aggregation.

The results presented in Figs. 3 and 4 show that the scaling exponents for this system cannot be universal. In order to understand this unexpected result we have investigated the motions of individual clusters in more detail. The complex motion of a cluster was simplified by considering only the motion of the central mass point of the cluster. There are effects that can change the position of the central mass point with nearly no motion of the cluster as a whole. For example, after the joining of two clusters a rearrangement of particles in the new cluster takes place [see the case (i) discussed above]. We assume that these disturbing changes are smaller than the influence of random local forces [case (iii)] that essentially contribute to the cluster motions. A very slow rotation of a cluster [case (ii)] does not change the position of the central mass point.

Cluster tracks shown in Fig. 5 (Fig. 6) were determined for the experimental data shown in Fig. 3 (Fig. 4). We see in Figs. 5 and 6 that the clusters moved in two directions; the

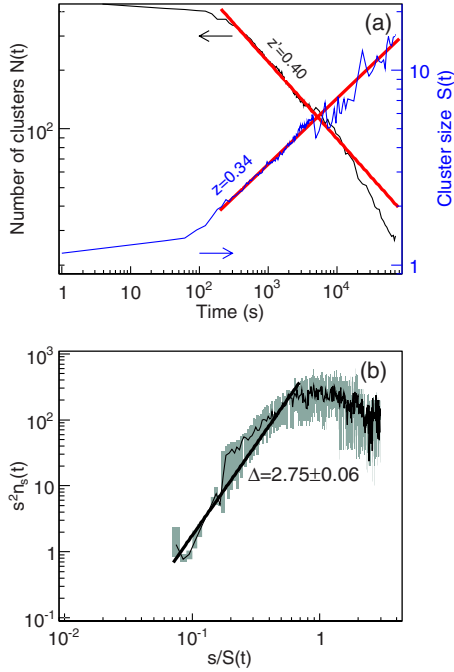


FIG. 4. (Color online) (a) The total number of clusters $N(t)$ and the mean (weight average) cluster size $S(t)$ (in units of number of spheres) versus time. (b) The universal scaling function $g(x) \sim x^{-\Delta}$ [$x = s/S(t)$, $x < 1$] calculated for the time interval $t = 200 - 80000$ s.

tracks are complex and show features of Brownian motion as expected.

For Brownian particles it is characteristic that their motion is well described by

$$\langle |\mathbf{r}(t)|^2 \rangle \propto Dt, \quad (3)$$

where $\mathbf{r}(t)$ is the distance vector between the initial position and particle position at time t and D is the diffusion coefficient. We checked the validity of Eq. (3) for the cluster tracks and determined the relation $D_s \propto \langle |\mathbf{r}(t)|^2 \rangle / t$ for all clusters of size s . For each experiment we analyzed about 1000 tracks

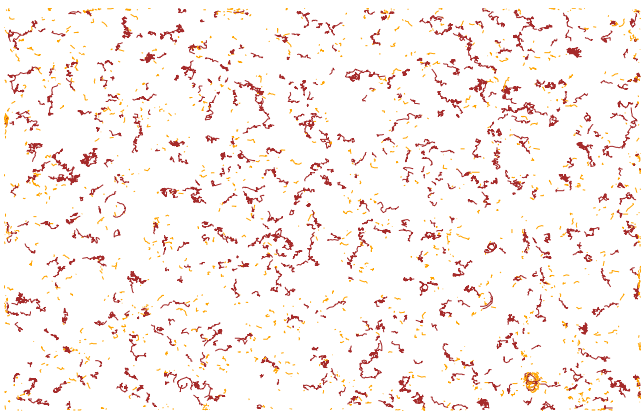


FIG. 5. (Color online) Tracks of particles and clusters in the experiment shown in Figs. 2 and 3 during the time interval $t = 0 - 3400$ s. Orange lines belong to short tracks that are shorter than 10 time steps (the time step $\Delta t = 30$ s). Brown tracks are longer than 10 time steps. The sample area is about $368 \times 274 \mu\text{m}^2$.

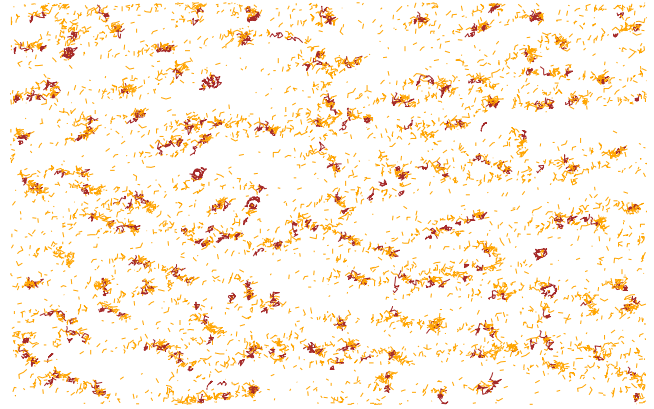


FIG. 6. (Color online) Tracks of particles and clusters during aggregation in the time interval $t = 0 - 3400$ s. Orange lines belong to short tracks that are shorter than 10 time steps (the time step $\Delta t = 30$ s). Brown tracks are longer than 10 time steps. The sample area is about $368 \times 274 \mu\text{m}^2$.

and found that this equation was valid with a cluster-size-dependent diffusion coefficient D_s .

We found that D_s clearly depended on the cluster size s as shown in Fig. 7. For the case in Fig. 7(b) the values of the diffusion coefficient D_s fall in a broad range covering nearly

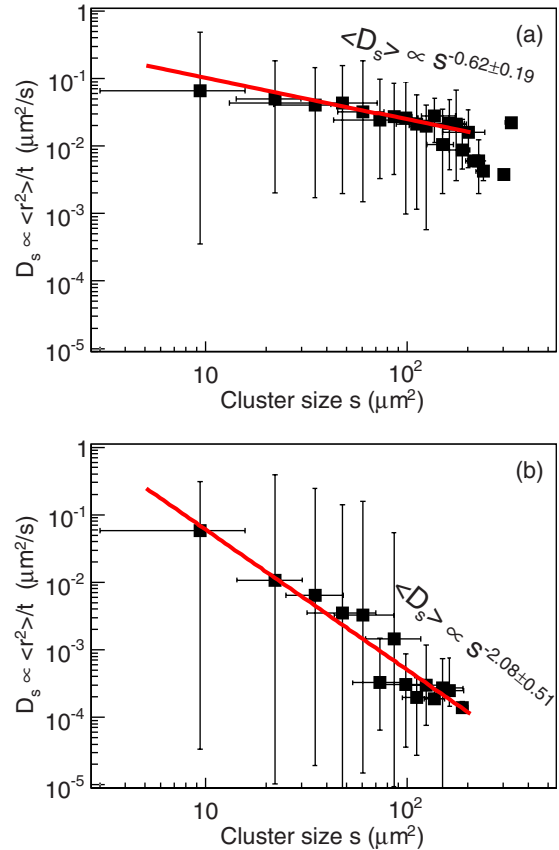


FIG. 7. (Color online) diffusion coefficients vs cluster size s . (a) For the experimental data shown in Figs. 3 and 5 the diffusion coefficient follows $\langle D_s \rangle \propto s^{-0.62 \pm 0.19}$. (b) For the experimental data shown in Figs. 4 and 6 the diffusion coefficient scales as $\langle D_s \rangle \propto s^{-2.08 \pm 0.51}$.

three decades. These ranges of values of D_s are significantly larger than possible errors of measurement. The average diffusion coefficient for cluster size $s\langle D_s \rangle$ was calculated, and the result (Fig. 7) was fitted to a scaling law $\langle D_s \rangle \propto s^\gamma$. For the data presented in Figs. 3 and 5 the diffusion scaling exponent $\gamma = -0.62 \pm 0.19$ was found. On the other hand, for the data in Figs. 4 and 6 the diffusion scaling exponent was clearly higher, $\gamma = -2.08 \pm 0.51$.

IV. DISCUSSION

We have observed that application of a rotating magnetic field on a 2D system of magnetic holes causes field-induced aggregation. The clusters move and can grow in both dimensions, which is different from the case of a constant magnetic field where clusters are free to move in both dimensions but grow only in one dimension as determined by the external magnetic field. The results show that the system was in a nonequilibrium state and its characteristic quantities, such as the number of clusters $N(t)$ and average cluster size $S(t)$, show scaling according to the cluster-cluster aggregation model [2] as shown in Figs. 3(a) and 4(a). Both the scaling properties and the broad cluster size distributions found, as well as the existence of a scaling function $g(x)$, are main signatures of cluster-cluster aggregation and dynamic scaling theory [4].

In many cases the cluster-cluster aggregation mechanism leads to formation of complex, fractal-like objects [1]. However, in the present case the structure of the aggregates was simpler, with a compact internal organization. Extremely slow cluster rotations and rearrangement of particles inside the new, bigger clusters were observed. As a consequence of these effects, the clusters were packed into regular objects with a nearly close-packed, triangular structure of the spheres. The cluster diffusion coefficients did not depend on the direction in which the clusters move, i.e., hydrodynamic corrections were not important as they were in the case of constant magnetic fields [9].

In the basic cluster-cluster aggregation model [2] it is assumed that the diffusion coefficient is $\gamma = -1$ and the corresponding scaling exponent is $z = 0.5$. We have determined two distinct values for the diffusion coefficients γ and scaling exponents z as a result of the two clearly different types of behavior observed in our experiments. The relationship between γ and z for both values of γ follows the equation $z = 1/(1-\gamma)$, which has been found in other aggregation models. For $\gamma = -0.62 \pm 0.19$ (-2.08 ± 0.51) we computed $z = 0.62$ (0.32). These scaling exponents agree well with exponents z determined directly from the time dependence of $S(t)$, $z = 0.64 \pm 0.01$ and 0.34 ± 0.02 , respectively.

Unfortunately, at present we are not able to explain why similar experiments on approximately the same samples (concentrations, layer thickness, etc.) show scaling exponents with values that come in two clearly separated ranges and diffusion exponents γ which are different from the expected value $\gamma = -1$. Thus, the scaling exponent z is clearly either lower or higher than the theoretically predicted value $z = 0.5$.

In an earlier study of a similar system of magnetic holes in a constant magnetic fields [8] it was found that for small

microspheres (diameters $d = 1.9\text{--}4.0 \mu\text{m}$ and interaction strength $\lambda = 8\text{--}370$) the scaling exponents z and z' were approximately equal, $z = z'$, and typically slightly lower than 0.5: $0.38 \leq z, z' \leq 0.54$. However, for larger particles, $d = 14 \mu\text{m}$ ($\lambda = 1040\text{--}10600$) the values of z and z' increased with the value of the dimensionless interaction strength λ from about 0.1 to 0.6, and correspondingly the value of Δ decreased from above 3.0 to ~ 1.5 . Thus, depending on the particle size, the scaling exponents changed from being nearly constant and near the theoretically expected values to being strongly nonuniversal. Although the present particles are within the diameter and λ ranges which showed nearly universal behavior in Ref. [8], the magnetic interactions are very different (anisotropic in the former and isotropic in the present) and thus the range of λ for which the behavior is nonuniversal seems to be changed.

It is unclear why the diffusion conditions, as quantified by the values of the diffusion coefficients γ , were so different in the two typical cases reported here. It may possibly be related to fine details in the interaction between the microspheres and the glass plates confining the system. In principle the magnetic holes should be repelled from the confining walls [10]. Thus, for particles of typical diameter of about half the plate separation, the apparent magnetic “image dipoles” created on both glass walls repel the magnetic holes and keep them near the center of the ferrofluid layer. However, there may be a slight shift of the position toward the upper plate due to the few percent higher density of the ferrofluid compared to that of the polystyrene microspheres [13]. For smaller spheres ($\sim 1/10$ plate separation) like those used in the current experiment, the situation should be exactly the same with the magnetic holes initially located near the center of the fluid layer as both buoyancy and magnetic forces are proportional to the volume of the particles. Since the diameters of the largest clusters obtained in these experiments were typically smaller than ten sphere diameters ($= 30 \mu\text{m}$), which is about half of the plate separation, it seems reasonable to assume that the hydrodynamic effects of the walls were negligible and thus that the clusters moved around as in bulk liquid. However, if a small fraction of the particles become attracted or even loosely attached to the walls, this will slow down the diffusion. Extremely small values of $\langle D_s \rangle$ could indicate that some of the particles are trapped in the sample volume or on the sample-glass boundary.

One may speculate that, if for some reason the actual layer thickness was considerably smaller than the nominal thickness $t \approx 50 \mu\text{m}$, one might expect a much stronger viscous coupling to the glass plates [16,17]. After a certain initial time, the typical length scale (or diameter) l of a cluster would be of the same size as the separation $h \sim t/2$ from the closest wall. In that case one might expect a viscous force on the cluster proportional to $(l^2/h)\eta v$ where v is the cluster velocity. Then the diffusion coefficient would be expected to approach $\gamma = -2$, as was found in the second example. However, such a large deviation from the nominal separation is unlikely since the spacer particles were quite stable, and it would easily have been seen as a change in the degree of transparency of the sample. On the other hand, aging effects of the confining glass plates, such as changes in their hydro-

philic properties or surface charge density, cannot be excluded and might have a similar effect of increasing the frictional forces and enforcing $\gamma \approx -2$.

V. CONCLUSIONS

Diffusion-limited cluster-cluster aggregation of magnetic holes has been induced by a rotating magnetic field. The main features of the experimental results were well described by a diffusion-limited cluster-cluster aggregation model and dynamic scaling theory. The experimental conditions were designed in an effort to have a well-defined model of a low-concentration many-body system where long-range interactions are dominant. At present, the reason that two main aggregation regimes were observed is not clear. This resulted in scaling exponent values clearly different from those predicted by theory for systems with short-range interactions. This difference in behavior was further confirmed by unusual

values of the scaling exponent γ of the diffusion coefficient that were found by cluster tracking. An open question remains: Why do the isotropic, long-range particle-particle interactions suppress the diffusion regime where the size dependence of the diffusion coefficient scales as $\gamma = -1$? This will hopefully be clarified in future studies.

ACKNOWLEDGMENTS

The authors thank Arne T. Skjeltorp for many stimulating discussions. The experimental part of this work has been done at the Institute for Energy Technology (IFE, Kjeller). J.C. thanks the Physics Department at IFE for kind hospitality. Visual data processing was realized using the results of the projects Nordugrid and KnowARC. We acknowledge financial support from the Slovak Ministry of Education Grant. No. 6RP/032691/UPJŠ/08. This work was supported by the Slovak Research and Development Agency under the contract No. RP EU-0006-06.

-
- [1] T. Vicsek, *Fractal Growth Phenomena*, 2nd ed. (World Scientific, Singapore, 1992).
 - [2] P. Meakin, *Phys. Rev. Lett.* **51**, 1119 (1983).
 - [3] M. Kolb, R. Botet, and R. Jullien, *Phys. Rev. Lett.* **51**, 1123 (1983).
 - [4] T. Vicsek and F. Family, *Phys. Rev. Lett.* **52**, 1669 (1984).
 - [5] P. Domínguez-García, S. Melle, J. M. Pastor, and M. A. Rubio, *Phys. Rev. E* **76**, 051403 (2007).
 - [6] G. Helgesen, A. T. Skjeltorp, P. M. Mors, R. Botet, and R. Jullien, *Phys. Rev. Lett.* **61**, 1736 (1988).
 - [7] J. Černák, *J. Magn. Magn. Mater.* **132**, 258 (1994).
 - [8] J. Černák, G. Helgesen, and A. T. Skjeltorp, *Phys. Rev. E* **70**, 031504 (2004).
 - [9] M. Carmen Miguel and R. Pastor-Satorras, *Phys. Rev. E* **59**, 826 (1999).
 - [10] A. T. Skjeltorp, *Phys. Rev. Lett.* **51**, 2306 (1983).
 - [11] G. Helgesen, P. Pieranski, and A. T. Skjeltorp, *Phys. Rev. Lett.* **64**, 1425 (1990).
 - [12] P. Pieranski, S. Clausen, G. Helgesen, and A. T. Skjeltorp, *Phys. Rev. Lett.* **77**, 1620 (1996).
 - [13] R. Toussaint, J. Akselvoll, G. Helgesen, A. T. Skjeltorp, and E. G. Flekkoy, *Phys. Rev. E* **69**, 011407 (2004).
 - [14] P. Tierno, R. Muruganathan, and T. M. Fischer, *Phys. Rev. Lett.* **98**, 028301 (2007).
 - [15] Type EMG 909, produced by Ferrotech, Nashua, New Hampshire.
 - [16] J. Mittal, T. M. Truskett, J. R. Errington, and G. Hummer, *Phys. Rev. Lett.* **100**, 145901 (2008).
 - [17] R. Di Leonardo, S. Keen, F. Ianni, J. Leach, M. J. Padgett, and G. Ruocco, *Phys. Rev. E* **78**, 031406 (2008).